17th World Conference on Earthquake Engineering, 17WCEE
Sendai, Japan - September 13th to 18th 2020
Paper N° C002482
Registration Code: S- A01972

UPPER AND LOWER BOUNDS OF DEVICE FORCE CAPACITY IN HIGH FORCE TO VOLUME (HF2V) DEVICE DESIGN

G.W. Rodgers[1], V. Vishnupriya[2], J.G. Chase [3], C. Zhou[4]

(1) *Professor, Department of Mechanical Engineering, Univ of Canterbury, Christchurch, New Zealand; geoff.rodgers@canterbury.ac.nz*
(2) *PhD Candidate, Department of Mechanical Engineering, Univ of Canterbury, Christchurch, New Zealand; vishnupriya.vishnupriya@pg.canterbury.ac.nz*
(3) *Professor, PhD Candidate, Department of Mechanical Engineering, Univ of Canterbury, Christchurch, New Zealand; Geoff.chase@canterbury.ac.nz*
(4) *Research Fellow, Department of Mechanical Engineering, Univ of Canterbury, Christchurch, New Zealand; cong.zhou@canterbury.ac.nz*

Abstract

To reduce seismic vulnerability and the economic impact of seismic structural damage, it is important to protect structures using supplemental energy dissipation devices. Several types of supplemental damping systems can limit loads transferred to structures and absorb significant response energy without sacrificial structural damage. Lead extrusion dampers are one type of supplemental energy dissipation devices. A smaller volumetric size with high force capacities, called high force to volume (HF2V) devices, have been employed in a large series of scaled and full-scaled experiments, as well as in three new structures in Christchurch and San Francisco.

HF2V devices have previously been designed using very simple models with limited precision. They are then manufactured, and tested to ensure force capacities match design goals, potentially necessitating reassembly or redesign if there is large error. In particular, devices with a force capacity well above or below a design range can require more testing and redesign, leading to increased economic and time cost. Thus, there is a major need for a modelling methodology to accurately estimate the range of possible device force capacity values in the design phase – upper and lower bounds.

Upper and lower bound force capacity estimates are developed from equations in the metal extrusion literature. These equations consider both friction and extrusion forces between the lead and the bulged shaft in HF2V devices. The equations for the lower and upper bounds are strictly functions of device design parameters ensuring easy use in the design phase. Two different sets of estimates are created, leading to estimates for the lower and upper bounds denoted $F_{LB,1}$, $F_{UB,1}$, $F_{UB,2}$, respectively. The models are validated by comparing the bounds with experimental force capacity data from 15 experimental HF2V device tests.

All lower bound estimates are below or almost equal to the experimental device forces, and all upper bound estimates are above. Per the derivation, the ($F_{LB,1}$, $F_{UB,1}$) pair provide narrower bounds. The ($F_{LB,1}$, $F_{UB,1}$) pair also had a mean lower bound gap of -34%, meaning the lower bound was 74% of device force on average, while the mean upper bound gap for $F_{UB,1}$ was +23%. These are relatively tight bounds, within ~±2 SE of device manufacture, and can be used as a guide to ensure device forces are in range for the actual design use when manufactured. Therefore, they provide a useful design tool.

Keywords: HF2V, lead dissipater; extrusion; energy dissipation; design

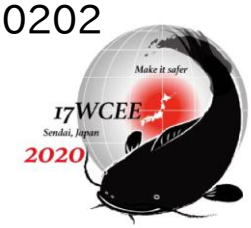

1. Introduction

Severe earthquakes subject structures to large energy inputs, due to ground motions causing significant structural response. Large motions lead to structural damage, and, in some cases, collapse. The cost associated with the repair, service disruption, and loss of infrastructure causes significant economic loss and can hinder long term economic development [1-3].

To mitigate social disruption and economic loss, and ensure life safety, supplemental earthquake damping systems can be used to control structural response during earthquakes. High Force to Volume (HF2V) lead extrusion dampers are supplemental dampers that dissipate energy by extruding lead in a closed container during ground motions [4, 5]. This damping method has found satisfactory applications in Christchurch rebuild with 96 applied in the Forté Health [6-8] and 20 more in the new Christchurch Library (Tūranga) [9]. They have also been validated in several test cases [10-22].

Extrusion is a forming process in which the working material is forced through a constricted area by an external load. Due to the inherent complexity of the extrusion process, exact prediction of extrusion forces can be difficult. Instead, most methods seek to approximate upper and lower limits on the extrusion forces [23-25]. There exist few design-based models able to accurately predict manufactured HF2V device forces precisely [26, 27]. Plain strain theory can be applied to metal forming processes with axisymmetric geometry for predicting approximate extrusion forces. It thus offers a potential route to creating accurate design models.

1.1. Bulk Extrusion Analogy

In direct extrusion processes, the ram moves forward to push the metal billet through the die, extruding the metal in the same direction. The metal is sheared and compressed between the dies to create plastic deformation to produce metal parts. The extrusion process in a HF2V device is a closed container operation, in which the working material can be repeatedly extruded by bulged shaft displacement.

More specifically, in a HF2V device, lead is plastically deformed during shaft motion and the working material is forced to flow against the shaft behind the bulge [4]. The working material remains within the containing cylinder after extrusion, regaining its mechanical properties through recrystallization behind the bulge [28] and does not cause changes in overall configuration of the working material in the HF2V devices, unlike metal forming extrusion processes. However, close analogies exist between the bulk extrusion processes and HF2V extrusion mechanisms, especially with the ‘constricted tube lead extrusion dampers’ [29, 30]. The constricted tube lead extrusion dampers are the early design of lead extrusion dampers, where bulged inner walls create an annular restriction through which lead is extruded. The HF2V devices are bulged shaft extrusion dampers, where lead is contained in a cylindrical housing and is deformed by axial motion of a centrally bulged shaft [30]. In comparison, the bulged shaft devices are cheaper to manufacture [31, 32] and hence more popular than the constricted type.

The analogical geometric parameters of bulk extrusion processes and HF2V lead extrusion dampers are given in Table 1 and represented in Fig. 1.

Table 1 – Analogous geometric parameters

HF2V parameters	Direct extrusion parameters
Cylinder	Container
Bulge	Die
Lead	Metal
Shaft	Ram

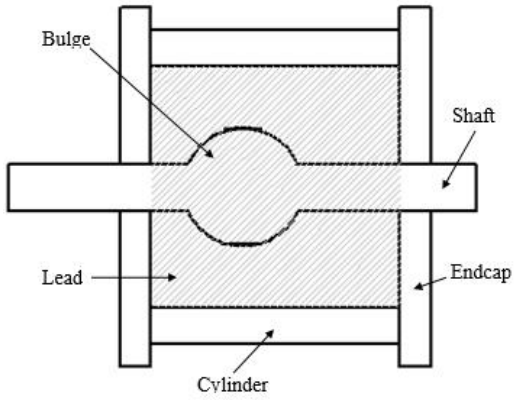

(a) HF2V configuration schematic

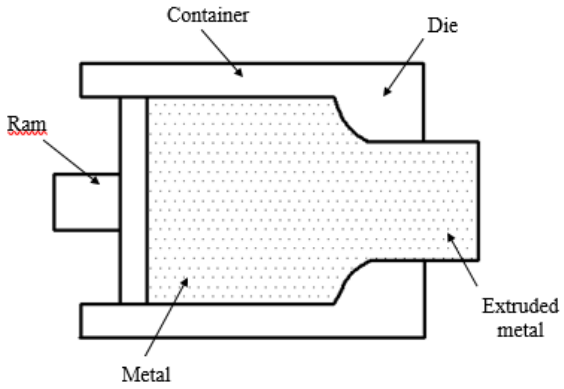

(b) Direct extrusion schematic

Fig. 1 – Key geometric parts in HF2V damper and Direct extrusion

2. Methods

To understand the operating mechanics of the HF2V devices better, the HF2V device parts are matched to direct metal extrusion processes to obtain upper bound (UB) and lower bound (LB) force capacities for the HF2V devices. The bulges of the HF2V damper are assumed to be on the walls, similar to the constricted tube extrusion damper, along with a no-bulge shaft, shown in Fig 2. In Fig. 2, L_{cyl} is cylinder length; L_{blg} is bulge length; $L_{flat\ bulge}$ is length of the flat surface of the bulge; d is the distance between the bulges; D_{cyl} is cylinder diameter; D_{sh} is the shaft diameter and α is the bulge angle. The endcaps are considered to operate similar to the ram in the direct extrusion process, extruding lead between the two bulges on the walls creating extrusion and friction forces. This analogy is expected to provide the same or similar forces to HF2V devices.

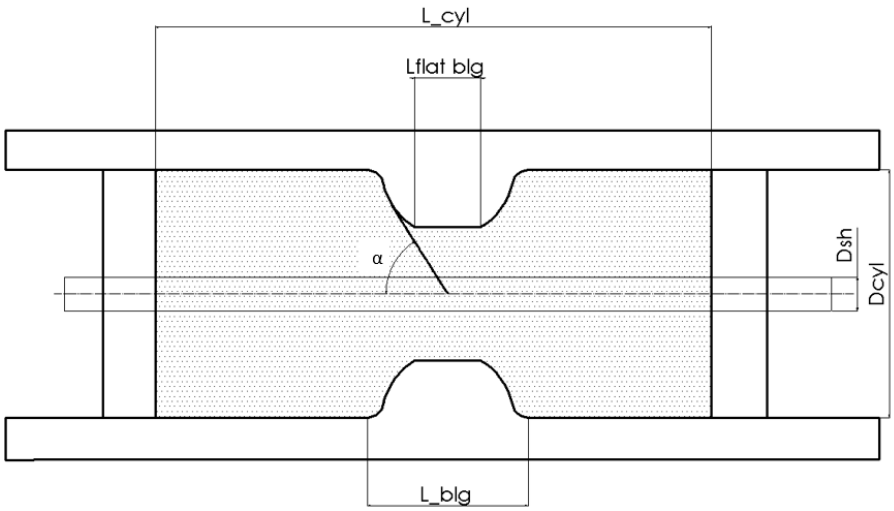

Fig. 2 - Direct extrusion geometry matched to HF2V devices.

2.1. HF2V UB modelling

A simplified, efficient upper bound (UB) extrusion solution for lead and aluminium alloys is considered in this analysis [33-35], independent of velocity fields and slip line fields [36]. The extrusion parameters are matched and applied to obtain a modified UB equation. The friction from endplates and the forces of compression of lead behind the bulge are not considered. The velocity of operation is considered as 0.5 mm/s for all the devices as the experimental tests previously undertaken were completed at this quasi-

static velocity. Due to the ambiguity regarding the forces due to wall friction as lead flows, two UB models are proposed.

2.1.1. Upper Bound Model 1 ($F_{UB,1}$)

Model 1 assumes intermetallic shear occurs in lead during the shaft displacement, shearing lead only along the shaft during displacement and the lead along the wall is not displaced [37]. Thus, there are no frictional forces from the cylinder walls, and all force is due to internal shear within the lead. However, the friction forces attained from friction between the lead and the shaft are captured in this model. A no bulge shaft is assumed and the frictional force produced along the entire shaft (F_f) is considered. The resulting model is defined:

$$F_{UB,1} = 2Y_o \frac{\pi\left(D_{cyl} - D_{sh}\right)^2}{4}\left[4\mu\left(\frac{L_{cyl}-L_{blg}}{D_{cyl} - D_{sh}} + \frac{L_{flat\ blg}}{D_{cyl} - D_{blg}}\right)\ln\left(\frac{D_{cyl} - D_{sh}}{D_{cyl} - D_{blg}}\right)^2\right] + F_f \quad (1)$$

Where, Y_o is the yield strength of lead, μ is the coefficient of friction between the lead and the steel shaft surface. As the friction forces produced at the cylinder walls are neglected in this equation, the minimum friction coefficient can be considered 0.05 between lead and walls for calculation [38, 39] of $F_{UB,1}$. The friction produced during interaction of lead and shaft (F_f) is given in Section 2.3.

2.1.2. Upper Bound Model 2 ($F_{UB,2}$)

Model 2 assumes friction forces are produced from the flow of lead along the cylinder walls during shaft displacement, thus contributing to overall HF2V device forces. Thus, UB Model 2 ($F_{UB,2}$) model accounts for the friction forces from lead-wall interaction [26, 27], defined:

$$F_{UB,2} = 2Y_o \frac{\pi\left(D_{cyl} - D_{sh}\right)^{\angle}}{4}\left[4\mu\left(\frac{L_{cyl}-L_{blg}}{D_{cyl} - D_{sh}} + \frac{L_{flat\ blg}}{D_{cyl} - D_{blg}}\right)\ln\left(\frac{D_{cyl} - D_{sh}}{D_{cyl} - D_{blg}}\right)^2\right] + F_{f\_sh} \quad (2)$$

Where, The friction coefficient at the lead-wall and lead-shaft interaction are considered as μ = 0.25 for $F_{UB,2}$ modelling [40, 41]. F_{f_sh} is the friction forces from the non-bulged section of the shaft as the friction forces along the bulged shaft have already been captured in the model given in Section 2.3.

2.2. HF2V Lower Bound Modelling (F_{LB})

Lower bound extrusion forces can be estimated based on work models used to obtain metalworking loads, which assumes homogenous deformation and zero friction [36, 42, 43]. The model assumes pure extrusion and can be used to estimate extrusion forces when the friction between the steel parts and lead is negligible. However, the LB model ($F_{LB,1}$) does consider the friction force developed at the shaft during extrusion. The LB force developed in the HF2V damper is defined:

$$F_{LB,1} = A_o Y_o' \ln\frac{A_o}{A_f} + F_f \quad (3)$$

Where, A_o is the area of lead before extrusion, A_f is the lead area after extrusion, and is defined:

$$A_o = \pi\frac{(D_{cyl} - D_{sh})^2}{4};\ A_f = \pi\frac{(D_{cyl} - D_{blg})^2}{4} \quad (4)$$

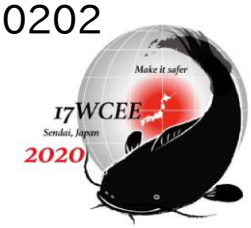

2.3. Friction Modelling

Accounting for frictional effects at the contact surface is complex and several studies have been undertaken to understand the mechanics involved at the contact boundary. A Coulomb friction based model is used to calculate friction forces from lead-shaft interface [44-47]. Thus, the frictional force component for the entire shaft is thus defined:

$$F_f = m\pi D_{sh} \frac{Y_o}{2} L_{cyl} \tag{5}$$

Where, m is the friction factor. The frictional force component when the friction contribution by the bulge is already captured is defined:

$$F_{f\_sh} = m\pi D_{sh} \frac{Y_o}{2} (L_{cyl} - L_{blg}) \tag{6}$$

The friction coefficient (μ) is μ = 0.25, and assumed constant at all points of interaction between the lead and shaft surface [40, 41].

3. Analysis

The UB and LB models in are applied to 15 HF2V lead extrusion dampers whose experimental test data and geometric dimensions are given in Table 2. The yield stress (Y_o) values are given in Table 3.

Table 2 – HF2V parameters used for UB and LB modelling

Devices	L_{cyl} (mm)	L_{blg} (mm)	D_{cyl} (mm)	D_{blg} (mm)	D_{shaft} (mm)	α (degrees)
1	110	30	89	40	30	68.2
2	110	30	89	50	30	51.3
3	110	30	89	58	30	41.8
4	130	30	66	40	30	68.2
5	130	30	66	50	30	51.3
6	50	23.3	50	32	20	56.8
7	70	20	50	32	20	56.3
8	100	30	50	35	24	66.3
9	160	20	60	42	33	62.1
10	100	23	50	35	24	59.9
11	75	30	70	48	30	54.2
12	160	20	54	35	30	73.6
13	160	20	54	36	30	70.6
14	160	20	54	38	30	64.8
15	100	17.2	40	27	20	65.3

The yield stresses (Y_o) for pure lead at different reduction percentages in compression at 20 °C is considered for HF2V devices [48]. The reduction percentage is the reduction in the area of lead at the bulge flat surface. The reduction percentage of lead between the bulge and the cylinder and their corresponding (Y_o) values are given in Table 3.

Table 3 - The yield stress values of pure lead from experimental tests [48].

Device	Percentage Reduction (%)	Y_o (N/mm^2)
1	17	23.17
2	34	29.30
3	47	32.43
4	28	27.80
5	56	33.91
6	40	32.43
7	40	32.43
8	42	32.43
9	33	30.89
10	42	32.43
11	45	32.43
12	21	26.26
13	25	27.03
14	33	30.89
15	35	31.00

The friction factor, m = 0.866, also known as the interface friction shear factor is a quantitative index for determining friction stresses at interface, calculated using the relationship [44, 49]:

$$m = 2\,\mu\sqrt{3} \tag{7}$$

A total of 15 HF2V experimental device forces (F_{exp}) are compared against the estimated upper bound and lower bound forces. The resulting UB and LB forces are compared to the peak forces from experimental tests. The experimental forces are expected to lie between the UB and LB forces. UB and LB models provide a rough estimation of a broad range of maximum and minimum expected forces from HF2V devices.

4. Results

Experimental HF2V device forces are compared to those calculated using the modified UB and LB estimates of equations (1) - (3) are compared in Fig. 3 and Table 4. Both UB values are larger than the experimental forces in all cases. The lower bound forces $F_{LB,1}$ are lower than all the experimental forces except Device 12, which is almost equal to the experimental force.

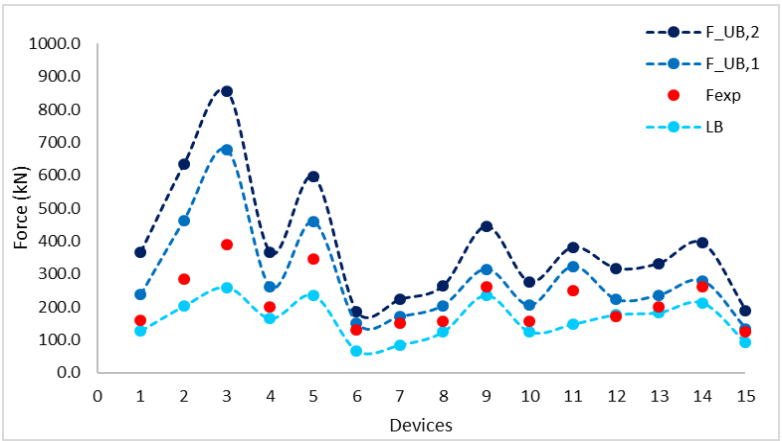

Fig. 3 - UB and LB force ranges for the HF2V devices

Table 4 - Comparison of HF2V LB and UB forces to Experimental forces

Devices	$F_{LB,1}$ (kN)	F_{exp} (kN)	$F_{UB,1}$ (kN)	$F_{UB,2}$ (kN)
1	126.8	160	236.7	366.2
2	201.5	285	463.4	634.4
3	258.6	390	676.4	856.3
4	164.8	200	259.7	364.7
5	234.4	346	458.1	596.9
6	67.2	130	149.3	184.9
7	84.7	150	170.1	222.2
8	124.0	155	203.7	263.7
9	234.6	260	314.7	444.8
10	124.0	155	204.6	275.6
11	147.2	250	322.6	381.5
12	175.7	170	222.2	317.0
13	182.2	200	235.5	332.3
14	211.5	260	278.8	394.1
15	92.1	125	134.2	189.7

The experimental forces (F_{exp}) are greater than the direct extrusion UB force values ($F_{UB,1}$ and $F_{UB,2}$) as expected, shown in Figure 3. $F_{UB,1}$ predictions, without the wall friction are closer to experimental test forces. The addition of wall friction makes the predictions of UB forces from $F_{UB,2}$ larger than $F_{UB,1}$ as expected. The $F_{UB,2}$ model over estimates the device forces by 30- 60%, while $F_{UB,1}$ over predicts forces by only 7- 42%. Thus, the $F_{UB,1}$ is a better choice for predicting the HF2V upper limit forces compared to $F_{UB,2}$ model. Hence, $F_{UB,1}$ and $F_{LB,1}$ model pair can be used to predict experimental device forces.

The $F_{UB,1}$ and $F_{LB,1}$ values provide limits of operational range of HF2V devices based on devices design parameters and deformation of lead in the devices by creating a tight bound for all devices except Devices 2, 3, and 5. Device 2, 3 and 5 have the largest diameters, which allows larger shearing of lead, consequently producing more heat, leading to greater variation in forces generated experimentally. To better understand the dependency of HF2V device forces and estimated UB and LB forces on the device parameters, the devices are plotted in Fig. 4 on basis of increasing values of device bulge diameter (D_{blg}).

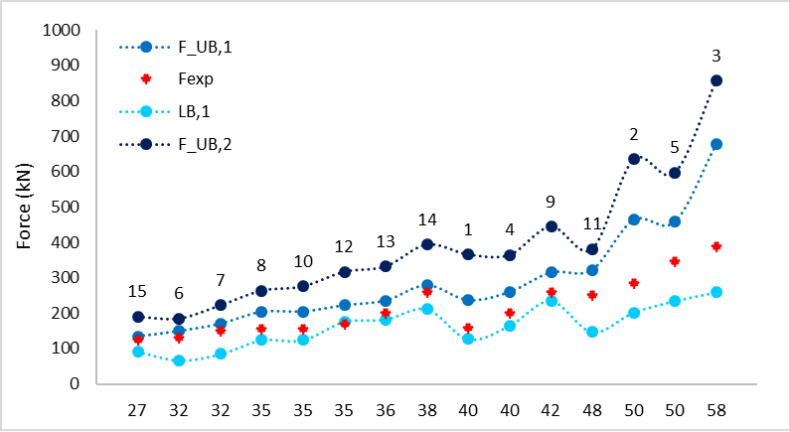

Fig. 4 – Devices ranked on increasing values of D_{blg}

Device forces, when sorted by increasing values of D_{blg}, shows almost a linear relationship between D_{blg} and HF2V device forces in Fig. 4. Hence, based on this plot, it can be deduced that D_{blg} values directly

influence HF2V device forces. A large bulge diameter induces larger strain or reduction percentage and deformation during loading, leading to production of large resistive forces [50]. Thus, the bulge diameter is a crucial parameter in determining the HF2V device force capacity. However, other factors directly influencing the total force exist [26, 27], which is why the plot is not monotonically increasing.

5. Conclusion

This paper has presented two upper bound (UB) and one lower bound (LB) force modelling methods for HF2V devices by relating direct extrusion parameters to HF2V lead extrusion devices. The UB models predict above the experimental force and the lower bound model predicts forces below or close to the experimental device forces with average gap of +23% and -34%. Bulge diameter is a key device design parameter influencing the HF2V device force output is identified in this study.

6. References

1. Abidi, S., S. Akbar, and F. Bioret. *Post-Event Reconstruction in Asia since 1999: An Overview Focusing on the Social and Cultural Characteristics of Asian Countries*. in *International Conference on Earthquake Engineering and Seismology*. 2011.
2. Parker, M. and D. Steenkamp, *The economic impact of the Canterbury earthquakes.* Reserve Bank of New Zealand Bulletin, 2012. **75**(3): p. 13-25.
3. Seville, E., J. Vargo, and I. Noy, *Economic recovery following earthquakes disasters.* Encyclopedia of Earthquake Engineering, 2014: p. 1-14.
4. Rodgers, G.W., *Next Generation Structural Technologies: Implementing High Force-to-Volume Energy Absorbers*, in *Mechanical Engineering*. 2009, University of Canterbury, Christchurch, New Zealand, Ph.D. thesis.
5. Rodgers, G.W., Denmead, C.S., Leach, N.C., Chase, J.G., Mander, J.B. *Experimental development and analysis of a high force/volume extrusion damper*. in *Proceedings New Zealand Society for Earthquake Engineering Annual Conference*. March 10-12, 2006. Napier, New Zealand.
6. Latham, D., A.M. Reay, and S. Pampanin. *Kilmore street medical centre: Application of a post-tensioned steel rocking system*. in *Steel Innovations Conference 2013*. 2013. Christchurch, New Zealand.
7. Latham, D.A., A.M. Reay, and S. Pampanin. *Kilmore Street Medical Centre: Application of an Advanced Flag-Shape Steel Rocking System*. in *New Zealand Society for Earthquake Engineering–NZSEE–Conference*. 2013. Wellington, New Zealand.
8. Rodgers, G.W., Chase, J.G.,Mander, J.B., *Repeatability and High-Speed Validation of Supplemental Lead-Extrusion Energy Dissipation Devices.* Advances in Civil Engineering, 2019. **Vol 2019**: p. 13.
9. Shannon, T. *Turanga Library Christchurch - Hybrid Rocking Precast Concrete Wall Panels*. in *Concrete New Zealand Conference*. 2019. Dunedin.
10. MacRae, G., C. Clifton, and S. Innovations. *Low damage design of steel structures*. in *Steel Innovations 2013 Workshop* 2013. Christchurch, New Zealand: Steel Construction New Zealand.
11. Rodgers, G., J. Mander, and J. Chase, *Full-Scale Experimental Validation of a DAD Post-Tensioned Concrete Connection Utilising Embedded High Force-to-Volume Lead Dampers*, in *New Zealand Society for Earthquake Engineering (NZSEE)* 2009: Christchurch
12. Bacht, T., Chase, J. G., MacRae, G., Rodgers, G. W., Rabczuk, T., Dhakal, R. P., & Desombre, J., *HF2V Dissipator Effects on the Performance of a 3 Story Moment Frame.* Journal of Constructional Steel Research, 2011. **67**(12): p. 1843 - 1849.
13. Rodgers, G.W., Mander, J.B, Chase, J.G, Dhakal, R.P, Leach N.C., Denmead, C.S., *Spectral Analysis and Design Approach for High Force-to-Volume Extrusion Damper-Based Structural Energy Dissipation.* Earthquake Engineering & Structural Dynamics, 2008. **37**(2): p. 207 - 223.
14. Rodgers, G.W., Solberg, K. M., Chase, J. G., Mander, J. B., Bradley, B. A., Dhakal, R. P., & Li, L. , *Performance of a Damage-Protected Beam-Column Subassembly Utilizing External HF2V Energy Dissipation Devices.* Earthquake Engineering & Structural Dynamics, 2008. **37**(13).

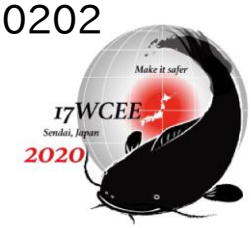

15. Rodgers, G.W., J.B. Mander, and J.G. Chase. *Full-Scale Experimental Validation of a DAD Post-Tensioned Concrete Connection Utilising Embedded High Force-to-Volume Lead Dampers*. in *New Zealand Society for Earthquake Engineering (NZSEE 2009)*. 2009. Christchurch.
16. Rodgers, G.W., Denmead, C., Leach, N., Chase, J.G., Mander, J.B. *Spectral Evaluation of High Force-Volume Lead Dampers for Structural Response Reduction*. in *Proc. New Zealand Society for Earthquake Engineering Annual Conference*. 2006. Napier, New Zealand.
17. Desombre, J.R., G.W.; MacRae, G.A.; Rabczuk, T.; Dhakal, R.P.; Chase, J.G., *Experimentally validated FEA models of HF2V damage free steel connections for use in full structural analyses.* 2011.
18. Rodgers, G.W., et al., *Beyond ductility: parametric testing of a jointed rocking beam-column connection designed for damage avoidance.* Journal of Structural Engineering, 2015. **142**(8): p. C4015006.
19. Mander, T.J., Rodgers, G.W., Chase, J.G., Mander, J.B., MacRae, G.A., Dhakal, R.P, *Damage avoidance design steel beam-column moment connection using high-force-to-volume dissipators.* Journal of structural engineering, 2009. **135**(11): p. 1390-1397.
20. Muir, C., D. Bull, and S. Pampanin. *Seismic testing of the slotted beam detail for reinforced concrete structures*. in *Structures Congress 2013: Bridging Your Passion with Your Profession*. 2013. Pittsburgh.
21. Muir, C.A., *Seismic performance of the slotted beam detail in reinforced concrete moment resisting frames*, in *Civil and Natural Resources Engineering*. 2014, University of Canterbury.
22. Wrzesniak, D., Rodgers, G.W., Fragiacomo, M, Chase, J.G., *Experimental Testing of Damage-Resistant Rocking Glulam Walls with Lead Extrusion Dampers.* Construction and Building Materials. **102**: p. 1145-1153.
23. Chen, C. and F. Ling, *Upper-bound solutions to axisymmetric extrusion problems.* International Journal of Mechanical Sciences, 1968. **10**(11): p. 863-879.
24. Adie, J. and J. Alexander, *A graphical method of obtaining hodographs for upper-bound solutions to axi-symmetric problems.* International Journal of Mechanical Sciences, 1967. **9**(6): p. 349-357.
25. Drucker, D., W. Prager, and H. Greenberg, *Extended limit design theorems for continuous media.* Quarterly of applied mathematics, 1952. **9**(4): p. 381-389.
26. Vishnupriya, V., et al., *Precision Design Modelling of HF2V Devices.* Structures, 2018. **14**: p. 243-250.
27. Vishnupriya, V., G.W. Rodgers, and J.G. Chase, *Precision Design Modelling of HF2V devices*, in *New Zealand Society of Earthquake Engineering Annual Conference (NZSEE 2017) and the AntiSeismic Systems International Society (ASSISI) 15th World Conference on Seismic Isolation, Energy Dissipation and Active Vibration Control of Structures*. 2017: Wellington, NZ.
28. Hofmann, W., *Lead and lead alloys*, in *Lead and Lead Alloys*. 1970, Springer. p. 25-320.
29. Robinson, W.H., *Cyclic energy absorber, US4117637 A*. 1978, Google Patents.
30. Robinson, W.H., Greenbank, L. R., *An Extrusion Energy Absorber Suitable for the Protection of Structures During an Earthquake.* Earthquake Engineering & Structural Dynamics, 1976. **4**(3): p. 251-259.
31. Robinson, W.H., *Recent research and applications of seismic isolation in New Zealand.* Bulletin-New Zealand National Society For Earthquake Engineering, 1995. **28**: p. 253-264.
32. Robinson, W., *Recent applications of high-damping hysteretic devices for the seismic isolation of buildings and bridges.* Journal of alloys and compounds, 1994. **211**: p. 592-595.
33. Tiernan, P., Hillery, M.T.,Draganescu, B.,Gheorghe, M., *Modelling of cold extrusion with experimental verification.* Journal of Materials Processing Technology, 2005. **168**(2): p. 360-366.
34. Pop, M., D. Frunza, and A. Neag, *Experimental and Numerical Aspects Regarding Lead Alloy Plastic Deformation.* Romanian Journal of Technical Sciences Applied Mechanics, 2012. **57**(1): p. 71-82.
35. Pop, M., Frunza, D., Neag, A., Pavel,C., *Researches on forward extrusion of lead alloy.* Metalurgia, 2012. **64**(1 : 10 - III).
36. Rowe, G.W., *Elements of metalworking theory*. 1979, London, UK: Hodder Arnold.
37. Saha, P.K., *Aluminum extrusion technology*. 2000: Asm International.
38. Lee, B., Y. Keum, and R. Wagoner, *Modeling of the friction caused by lubrication and surface roughness in sheet metal forming.* Journal of materials processing technology, 2002. **130**: p. 60-63.
39. Yoo, S.-S. and D.-E. Kim, *Minimum lubrication technique using silicone oil for friction reduction of stainless steel.* International Journal of Precision Engineering and Manufacturing, 2013. **14**(6): p. 875-880.

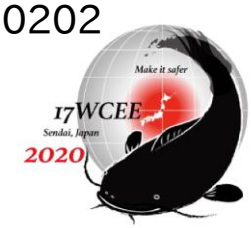

40. Zhou, Y., *Lead 65: Edited Proceedings, Second International Conference on Lead, Arnhem*. 2014: Elsevier Science.
41. Bowden, F.P. and L. Leben, *The nature of sliding and the analysis of friction.* Proceedings of the Royal Society of London. Series A. Mathematical and Physical Sciences, 1939. **169**(938): p. 371-391.
42. Symons, D.D., J. Chen, and P. Alton, *Calculation of optimal jaw geometry for an electronic bond pull test.* Proceedings of the Institution of Mechanical Engineers, Part C: Journal of Mechanical Engineering Science, 2014. **228**(11): p. 1847-1858.
43. Horrobin, D. and R. Nedderman, *Die entry pressure drops in paste extrusion.* Chemical Engineering Science, 1998. **53**(18): p. 3215-3225.
44. Bakhshi-Jooybari, M., *A theoretical and experimental study of friction in metal forming by the use of the forward extrusion process.* Journal of materials processing technology, 2002. **125**: p. 369-374.
45. Dongare, V.S., *Hot Extrusion of Carbon Nanotube-Magnesium Matrix Composite Wire*. 2014, Ohio University.
46. DePierre, V. and F. Gurney, *A method for determination of constant and varying friction factors during ring compression tests.* Journal of Lubrication Technology, 1974. **96**(3): p. 482-487.
47. Velu, R. and M. Cecil, *Quantifying Interfacial Friction in Cold Forming using Forward Rod Backward Cup Extrusion Test.* Journal of The Institution of Engineers (India): Series C, 2012. **93**(2): p. 157-161.
48. Loizou, N., Sims, R.B., *The yield stress of pure lead in compression.* Journal of the Mechanics and Physics of Solids, 1953. **1**(4): p. 234-243.
49. Molaei, S., M. Shahbaz, and R. Ebrahimi, *The relationship between constant friction factor and coefficient of friction in metal forming using finite element analysis.* Iranian Journal of Materials Forming, 2014. **1**(2): p. 14-22.
50. Pearson, C.E. and R.N. Parkins, *The Extrusion of Metals*. 1960: Chapman & Hall.

